KfK 3555
November 1983

Local Density Approximation in Effective Density-Dependent αN-Interactions

H. J. Gils
Institut für Kernphysik

Kernforschungszentrum Karlsruhe

KERNFORSCHUNGSZENTRUM KARLSRUHE

Institut für Kernphysik

KfK 3555

LOCAL DENSITY APPROXIMATION IN EFFECTIVE DENSITY-DEPENDENT αN-INTERACTIONS

H. J. Gils

Kernforschungszentrum Karlsruhe GmbH, Karlsruhe

Kernforschungszentrum Karlsruhe GmbH
ISSN 0303-4003

Abstract

Different forms of a local density approximation (LDA) in effective density-dependent αN-interactions are compared in single-folding optical model analyses of elastic α particle scattering by $^{40,42,44,48}Ca$ at E_α=104 MeV and by ^{40}Ca at E_α = 140 MeV. It is shown that the form of the LDA considerably influences the results on folded optical potentials. A variable form of the LDA is suggested and discussed which includes previous forms as limiting cases. The new form leads to better fits to the data and to full consistency with the best available "model-independent" optical potentials.

LOKALE DICHTE-NÄHERUNG
IN
EFFEKTIVEN DICHTEABHÄNGIGEN
αN-WECHSELWIRKUNGEN

Zusammenfassung

Verschiedene Formen einer lokalen Dichte-Approximation (LDA) für eine dichteabhängige effektive αN-Wechselwirkung werden in Faltungsmodellanalysen der elastischen α-Teilchen-Streuung an $^{40,42,44,48}Ca$ bei E_α=104 MeV und an ^{40}Ca bei E_α=140 MeV verglichen. Es wird gezeigt, daß die Form der LDA die Faltungspotentiale deutlich beeinflußt und daß die früher häufig angenommene Äquivalenz verschiedener Formen nicht erfüllt ist. Es wird eine neue Form der LDA vorgeschlagen und diskutiert, die frühere Formen als Grenzfälle enthält, jedoch deren Unzulänglichkeiten vermeidet. Die vorgeschlagene LDA führt zu einer besseren Beschreibung der experimentellen Daten und die Faltungspotentiale sind vollkommen konsistent mit "modell-unabhängigen" empirischen Potentialen.

1. Introduction

Single- and double-folding models of the real optical potential for nucleon, light and heavy ion scattering have successfully been applied to the analysis of elastic and inelastic scattering cross sections [1-10 and further references cited therein]. The results in general demonstrate that folding models provide a relevant microscopic interpretation of the scattering process in particular for α particle scattering where a large basis of experiments is available. In many cases [1-2, 4-7, 9,10] the nuclear structure informations (size and shape of nuclear densities) needed for the folding procedure were adopted from independent sources and the effective projectile-nucleon interaction was subject of the studies, i. e. the importance of different effects like antisymmetrization or density-dependence to be explicitly included into the folding model approach. On the other hand, the folding models offer the possibility to extract nuclear properties from experimental cross sections if the effective interaction is reliably known. As in the studies of the reaction mechanism [1-2, 4-7, 9,10] also in this reversal use of the folding model [3, 8] the most important criteria for the relevance of the results are the questions how good do the folded optical potentials reproduce the phenomenological ones and how good is the description of the experimental cross sections, as characterized by the value of χ^2/F (χ^2 per degree of freedom), compared to the best value attainable with phenomenological procedures. The answers to these questions, however, strongly depend on the ingredients of the effective interaction used. Hence, investigations of the latter are a necessary precondition for a reliable determination of nuclear properties by use of folding models.

2. Background and Motivation

In the present paper we study particular aspects of the density-dependence of the effective interaction in folding model analyses of elastic α particle scattering at energies around E_α = 100 MeV. The work was performed as a pre-step for further analyses aiming at the determination of nuclear structure by use

of the approaches suggested below. We also emphasize that the semi-phenomenological approach adopted here should not, in principle, compete with more fundamental treatments of effective interactions (except of the χ^2-criterion in representing experimental data). Background of the studies is the fact that recently precise experimental data of elastic α particle scattering became available for a series of neighbouring nuclei [11, 12]. These cross sections enable an unambiguous very accurate determination of the real optical potentials in particular when introducing flexible so-called "model-independent" potential forms like the Fourier-Bessel (FB) method [11, 13] yielding an excellent representation of the experimental data as demonstrated by values of χ^2/F close to 1. Even minor effects of the real potentials like differences in size and shape between neighbouring nuclei are revealed by these data and methods [11]. Consequently, it is near by hand, to interprete the potential differences in terms of nuclear densities by use of folding models. The measure of relevance for such studies is provided by the "model-independent" potentials which represent the best description possible of the experimental data in terms of a complex optical potential. Since the model-independent FB-potentials enable to determine realistic errors of the radial shape of the potential and of its various radial moments [11, 13] there are well-defined criteria given for comparing folded potentials with the corresponding phenomenological ones. If the folding model results are found to be inside these error bands or to exceed them only slightly and if the value of χ^2/F also approaches the phenomemenological one closely the results of the folding analyses can be accepted with great confidence. One should note that these well-defined criteria are much sharper than previous ones based on the comparison with constrained potentials (e.g. Woods-Saxon (WS) form) which do not provide realistic estimates of errors and which yield a considerably poorer description of experimental cross sections [11]. On this level of improved accuracy, however, the criteria were not by far fulfilled previously, neither by the most advanced double-folding models based on fundamental NN-interactions [6, 10] nor by single-folding models based on phenomenologically determined αN-interactions [8] (which usually yield better results).

In particular the failure of double-folding models [5,6,10], which usually are assumed to be the preferrable approach for composite projectile scattering is remarkable. For heavy ion scattering this assumption must certainly be accepted since the double-folding models treat the interacting nucleons of target and projectile on equal footings and most of them do so also for the densities [9]. With regard to the density-dependence of the effective NN-interactions used, one may, however, doubt whether this symmetric treatment of target and projectile can be transferred to the case of α particle scattering without any change. The density of α particles is three times larger than those of heavier nuclei and is close to the density of a proton (assuming Gaussian shape for both). Also the size of the α particle is close to that of a proton and its binding energy is much higher than those of heavier nuclei. These facts may have a considerable influence on the density-dependence of the NN-interaction used for double-folding model analyses of α particle scattering and may partly explain the discrepancies between double-folding potentials and the corresponding model-independent ones.

In single-folding optical potentials of α particle scattering the projectile is assumed to be a point particle (like the interacting target nucleons) and effects due to the finite size and density of the α particle (which anyway are not subject of such studies) are implicitly included in the form factor of the effective interaction. This form factor is a function of the distance between the α particle and the target nucleon only (i.e. independent of the target density) and it may be determined directly from α particle scattering cross sections [3,8,12]. Considering the values of the size and density of the α particle this simplification seems quite reasonable as also demonstrated by many single-folding analyses [1-3,8,12], in particular, because it avoids - by treating the projectile in a phenomenological way - the general problems of α particle double-folding models discussed before. However, when comparing single-folding potentials with "model-independent" phenomenological ones there are also some discrepancies [8,12], which may be due to the particular prescription of the density-dependence of the effective αN-interaction.

The study of this question is subject of the present work the experimental basis of which are the elastic scattering cross sections by $^{40,42,44,48}Ca$ at E_α = 104 MeV from the Karlsruhe group [11]. These data were measured in exceptionally small angular steps (0.25° - 0.5°) and extend over a large angular range ($3° \leq \theta_{CM} \leq 120°$) covering nine orders of magnitude in the cross sections. In order not to rely on possibly accidental results at one projectile energy experimental data for ^{40}Ca at E_α = 140 MeV from Maryland [14] have also been included into the analyses. This angular distribution (containing 44 data points as compared to 160 in the case of the 104 MeV data) covers six orders of magnitude in the cross sections with angular steps of 0.75° in the diffraction region.

3. Methods

In the single folding model for α-nucleus scattering the real part of the optical potential is written as

$$- \mathrm{Re}\, U(r_\alpha) = \int V_{\alpha N}(\vec{r}_N, \vec{r}_\alpha, \rho_m) \cdot \rho_m(\vec{r}_N) \cdot d\vec{r}_N \qquad (1)$$

where $\rho_m(r_N)$ is the target (point) nuclear matter density normalized to the number of nucleons A and $V_{\alpha N}(\vec{r}_N, \vec{r}_\alpha, \rho_m)$ is an effective α-nucleon-interaction. If the experimental data range to large scattering angles as in the present case, it was found [8] that the effective interaction has to be density-dependent. Following previous descriptions [4,8-10] $V_{\alpha N}$ is assumed to be factorized into a density independent part $f(\vec{x})$ depending only on the distance $|\vec{x}| = |\vec{r}_N - \vec{r}_\alpha|$ between the α particle and the interacting nucleon and a density-dependent part $v_{DD}(\rho_m)$.

$$V_{\alpha N}(\vec{r}_N, \vec{r}_\alpha, \rho_m) = f(|\vec{x}|) \cdot v_{DD}(\rho_m) \qquad (2)$$

As radial form factor $f(\vec{x})$ we use for convenience a Gaussian plus Yukawa form [12,15]

$$f(|\vec{x}|) = V_G \cdot \exp(-|\vec{x}|^2/a_G^2) + V_Y \cdot \exp(-|\vec{x}|/a_Y)/(|\vec{x}|/a_Y) \qquad (3)$$

The density-dependence for NN- and αN-interactions is in the

literature alternatively parametrized as [4-10, 16-18]

$$v_{DD}(\rho_m) = \lambda \cdot [1 - \gamma \rho_m^{2/3}] \tag{4a}$$

$$v_{DD}(\rho_m) = \lambda \cdot [1 + \gamma \exp(-\beta\rho_m)] \tag{4b}$$

with the normalization factor λ usually taken to be 1.

Using suitable parameters γ, β these forms were previously found to be (more or less) equivalent. These findings were confirmed in the present work and a preference of one of these approaches will not further be discussed. In the following we use the form (4a) for which it has been shown by analytical derivations [19] and phenomenological studies [20] that it reproduces the gross dependence on target mass number and projectile energy of the real optical α-nucleus potential over wide ranges. Rather than the analytical parametrization (4a,b) of the density-dependence the subject of the present investigation is the question, which *local* density $\rho_m(\vec{r})$ (i.e. the local density ρ_m at what space coordinate $\vec{r}$) has to be used in eq. 4 (LDA). From the theoretical point of view [17] there is no à priori preference for any particular form of the LDA. For practical purposes most frequently the forms

$$v_{DD}^{N}(\rho_m) = \lambda \cdot [1 - \gamma \rho_m^{2/3}(\vec{r}_N)] \tag{5a}$$

$$v_{DD}^{N\alpha/2}(\rho_m) = \lambda \cdot [1 - \gamma \rho_m^{2/3}(\frac{\vec{r}_N+\vec{r}_\alpha}{2})] \tag{5b}$$

have been used and were assumed to be equivalent due to the short range of $f(|\vec{x}|)$ in particular for NN-interactions ($\vec{r}_\alpha = \vec{r}_N$ is, in this case, the coordinate of the projectile nucleon) [4-7, 9,10]. If this assumption (being true for zero range interactions $f(|\vec{x}|) \equiv \delta(|\vec{x}|)$) is resonable, then also the form

$$v_{DD}^{\alpha}(\rho_m) = \lambda \cdot [1 - \gamma \rho_m^{2/3}(\vec{r}_\alpha)] \tag{5c}$$

should be equivalent to eqs. 5a, b. Whether this is the case for effective αN-interactions which have a rather large range will be investigated in the following by a direct comparison of these three cases (5a-c) in describing experimental data.

In order to get a further insight into the changes of the optical potential between the two extreme forms of the LDA (eqs. 5a and c) we suggest a form of the LDA which allows a continuous change between eq. 5a and eq. 5c and also approaches eq. 5b without making the folding integral complicated, namely

$$v_{DD}^{M}(\rho_m) = \lambda \cdot [1-m\gamma\rho_m^{2/3}(\vec{r}_N)]\,[1-(1-m)\gamma\rho_m^{2/3}(\vec{r}_\alpha)] \qquad (6)$$

For m = 1 this form is exactly equal to eq. 5a and for m = 0 it is equal to (5c). For m = 0.5 it closely approaches (5b) (see below). We call this form "mixed" LDA (superscript M).

4. Results

a) Calibration of the Effective Interaction

For the comparison of the different forms of the LDA (eqs. 5a-c, 6) with experiment we used the example ^{40}Ca (α,α) at E_α = 104 MeV as calibration nucleus for the effective interaction. For this purpose the nuclear matter density ρ_m calculated by Brown et al. [21] was chosen whose calculations reproduce very well the experimentally determined charge distribution of ^{40}Ca and the result of Hartree-Fock calculations for the neutron distribution. The parameters V_G, a_G, V_Y, γ (eqs. 3, 4a) were varied in a fit to the data together with the imaginary part of the optical potential which was of the Woods-Saxon (WS) shape. The parameter a_Y was adjusted in such a way that the root-mean-square (rms) radius of the folded real potential approximately reproduced the phenomenological value found in "model-independent" analyses using a FB real potential [11, 13]. The analyses were performed with modified versions of the Karlsruhe optical model code MODINA [22]. The results are compiled in Table 1a, b together with characteristic quantities of the phenomenological FB-potential for comparison. Also shown are the values of χ^2/F characterizing the goodness of the fit. Table 1 clearly indicates that the different forms of the LDA are not equivalent in fitting the data and reproducing the characteristic quantities of the

phenomenological real potential. In particular the correct value of the specific volume integral $-J_V/4A$ is closely met only by the forms (5c) and (6) with the value m = 0.2. One should also note that the errors of the parameter values obtained from the fits are considerably smaller in the case (6) as compared to all of the other approaches.

The "mixed" LDA (eq.6) is in detail studied in Fig. 1 where the parameter values V_G, a_G, V_Y, a_Y and γ obtained from fits to the ^{40}Ca cross sections are plotted versus the mixing parameter m. In the lower part of Fig. 1 the corresponding values of χ^2/F are also shown. After a region of constant χ^2/F ranging from m = 0 up to m $\approx$ 0.4 an increase of χ^2/F is observed confirming the findings from Table 1. The parameters of the density-independent part $f(|\vec{x}|)$ (eq. 3) show little variation in the region of constant χ^2/F with a vanishing gradient at m $\approx$ 0.2. In contrast, the parameters of $f(|\vec{x}|)$ vary dramatically for m $\gtrsim$ 0.4, the region of increasing χ^2/F. Similar features are observed for the correlation between γ and m which is linear for m $\lesssim$ 0.4 and extremely non-linear beyond. The remarkable feature of a vanishing variation of *all* parameters of $f(|\vec{x}|)$ for m $\approx$ 0.2 means that for this value of m the density-independent part $f(|\vec{x}|)$ and the density-dependent part $v_{DD}(\rho_m)$ are completely uncorrelated. Together with the small parameter errors this is an important confirmation for the hypothesis of $V_{\alpha N}$ being factorizable into these two parts (eq. 2). One should note that such a direct proof of this factorization hypothesis by fitting precise experimental data under slightly varying conditions has not been given before. Considering also the minimum value of χ^2/F the "mixed" LDA with m = 0.2 is found to be most reasonable in describing the elastic α particle scattering by ^{40}Ca. The corresponding value of γ = 1.645 fm^2 is in excellent agreement with the value γ = 1.65 fm^2 found in Hartree-Fock calculations with a local density-dependent NN-interaction [17].

One can speculate that the "mixing" value m = 0.2 is related to the ratio of nucleon numbers (1:4) of the interacting particles. However, one should avoid in this context to stress the folding model so strong and should regard this relation to be accidental.

Table 1a Parameters of the effective αN-interaction obtained from analysis of $^{40}Ca(\alpha,\alpha)$ at E_α = 104 MeV using different forms of the LDA

LDA eq.	χ^2/F	V_G (MeV)	a_G (fm)	V_Y (MeV)	a_Y (fm)	γ (fm^2)	m
5a	3.3	50.8 ± 1.7	1.797±0.0078	57.±4.4	1.0	2.136 ± 0.021	-
5b	2.9	21.4 ± 1.2	1.926±0.013	162.±6.6	0.83	1.800 ± 0.023	-
5c	2.6	19.1 ± 1.1	2.020±0.014	102.±5.6	0.86	1.382 ± 0.024	-
6	2.6	20.6 ± 0.6	2.009±0.0064	111.±1.8	0.85	1.645 ± 0.018	0.2

Table 1b Volume integrals J and radial moments of the folded real optical potentials and of the WS imaginary potential as compared to the phenomenological FB-potential

LDA eq.	χ^2/F	$-J_V/4A$ (MeV fm³)	$\langle r^2\rangle_V^{1/2}$ (fm)	$\langle r^4\rangle_V^{1/4}$ (fm)	$\langle r^6\rangle_V^{1/6}$ (fm)	$-J_W/4A$ (MeV fm³)	$\langle r^2\rangle_W^{1/2}$ (fm)
FB	2.2	325 ± 3	4.35 ± 0.02	4.83 ± 0.03	5.28±0.05	103.	4.93
5a	3.3	317.	4.35	4.86	5.34	99.	4.94
5b	2.9	318.	4.35	4.85	5.30	101.	4.92
5c	2.6	321.	4.35	4.84	5.29	102.	4.92
6	2.6	320.	4.35	4.84	5.29	102.	4.91

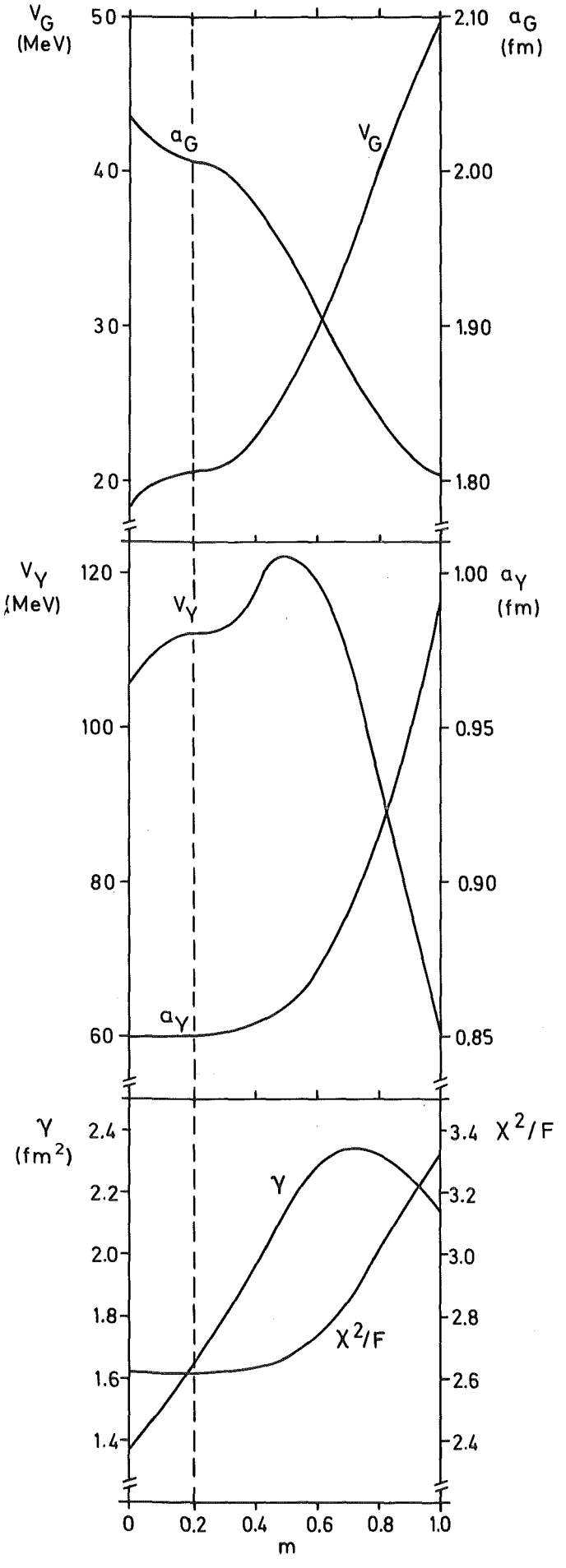

Fig. 1 Variation of the parameters of the effective αN-interaction (eqs. 3,6) over the "mixing" parameter m and corresponding values of χ^2/F.

The parameter values of the effective interaction and the corresponding characteristic quantities of the folded optical potentials for m = 0.2 are included in Table 1a, b (line 4) the latter showing up a good agreement with the phenomenological FB-potential.

The shapes of the effective αN-interactions obtained with the different forms of the LDA are compared in Fig. 2. The interacting target nucleon was assumed to be placed at three characteristic radial positions of different density in the ^{40}Ca nucleus, as indicated in the upper part of Fig. 2. (For simplicity, we used the Fermi-form for ρ_m having the same rms-radius as the more realistic density ρ_m from Ref. 21 used in the analyses of the cross sections). The outermost parts on the right hand side of Fig. 2 show the shape of the density-independent part $f(\vec{x})$ (eq. 3) ($\rho_m(r_N) \equiv \rho_m(r_\alpha) \equiv 0$) for each form of the LDA. The quoted values of the specific volume integrals J/4 indicate considerable variations of this quantity. Only the suggested "mixed" LDA approaches the theoretically expected value of about $J_v/4$ = 380 MeV fm^3 [18,23], The shapes of the free αN-interactions also differ from each other in particular in the radial region between $\vec{x} = |\vec{r}_N - \vec{r}_\alpha|$ = 1 fm and 3 fm which is most sensitive to the analyses. The rms-radii quoted in Fig. 2 may be compared with the value determined from the rms-radii of the best-fit phenomenological FB-potential $\langle r^2_{pot}\rangle^{1/2}$ and of the nuclear matter density $\langle r_m^2\rangle^{1/2}$ assuming a density-independent effective interaction

$$\langle r^2\rangle^{1/2} = (\langle r^2_{pot}\rangle - \langle r_m^2\rangle)^{1/2} = 2.74 \text{ fm} \qquad (7)$$

Due to the ignored density-dependence this value is much larger than the corresponding ones of all of the different folding approaches (eqs. 5a-c, 6), as expected.

The outermost left hand graphs show the shapes of the effective interactions when both the interacting nucleon and the α particle are embedden in nuclear matter of the density ρ_m = 0.168 fm^{-3}. In this case the effective interaction on the basis of LDA 5a which - as the only one - does not consider the density at the position of the α particle deviates remarkably from the other approximations at small radii. The graphs in the middle of Fig. 2 display the interactions for the case of the inter-

acting nucleon being placed in a density region corresponding to the nuclear surface and the density at the position of the α particle varies according to the density ρ_m as shown on top of Fig. 2. It is obvious from Fig. 2 that the LDA of the form 5a frequently used in the past yields an effective interaction which is too strong at the nuclear surface and too weak in the interior. The same holds also for eq. 5b but less pronounced. The effective interactions obtained with eqs. 5c and 6 are rather similar as expected from the value m = 0.2.

One may be also interested in the question, how the parameters λ (which was fixed to $\lambda = 1$ so far) and γ of the density-dependent part v_{DD} may change for different forms of the LDA (varying m) if the density-independent part $f(\vec{x})$ is kept fixed. This is demonstrated in Fig. 3 together with the corresponding values of χ^2/F. Again, we observe a linear correlation between the parameters for $0 \leq m \lesssim 0.4$ accompanied by a flat χ^2/F-minimum indicating equivalent description of the experimental data in the ranges $\lambda = 0.95 - 1.05$ and $\gamma = 1.42 - 1.86$ fm^2.

b) Description of Different Nuclei at Different Energies

In order to see whether the above findings concerning the LDA are also valid for other nuclei the parameters of the density-independent part of $V_{\alpha N}$ were kept fixed as obtained from the 'calibration nucleus' ^{40}Ca (Table 1a). When doing so one should keep in mind that these parameters are also closely related to the nuclear matter density ρ_m [21] adopted to be the 'true' density. When furtheron analyzing the differential cross sections of other target nuclei adopting the corresponding nuclear densities from the same source [21] one must be confident that these nuclear densities as well represent the 'true' densities as in the case of ^{40}Ca. This is not á priori given and can not easily be proven experimentally due to the well known difficulty in investigating the neutron distributions in nuclei. In fact, there are indications [12,24] that this assumption is not perfectly met by the adopted densities in particular not for ^{48}Ca. Nevertheless, we proceed using the densities calculated by Brown et al.[21] in order to avoid confusion e.g. by mixing experimental densities into this step of the analysis. The results on

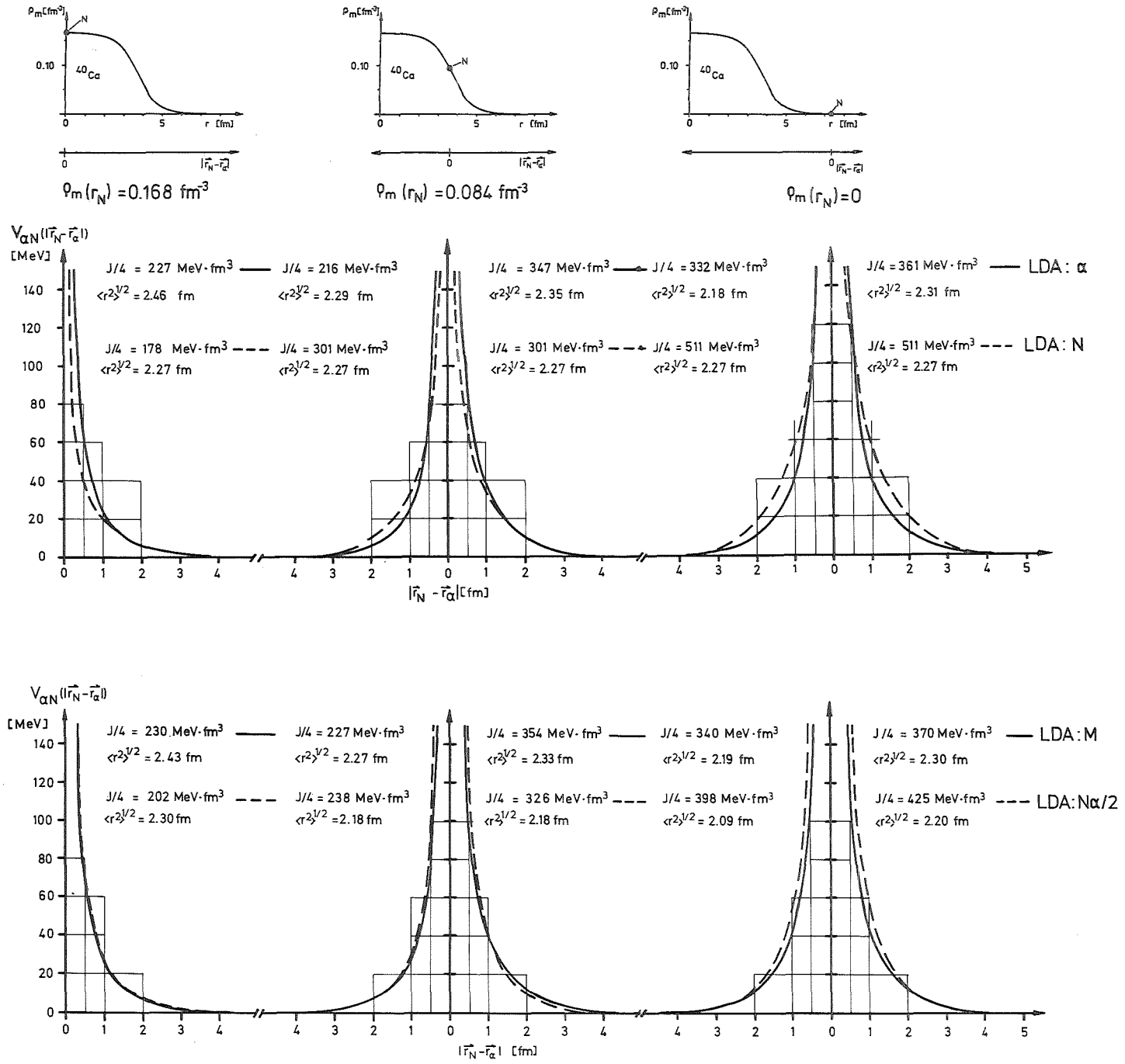

Fig. 2 Radial shapes, specific volume integrals J/4 and rms-radii of the effecitve αN-interactions as obtained with different forms of the LDA.

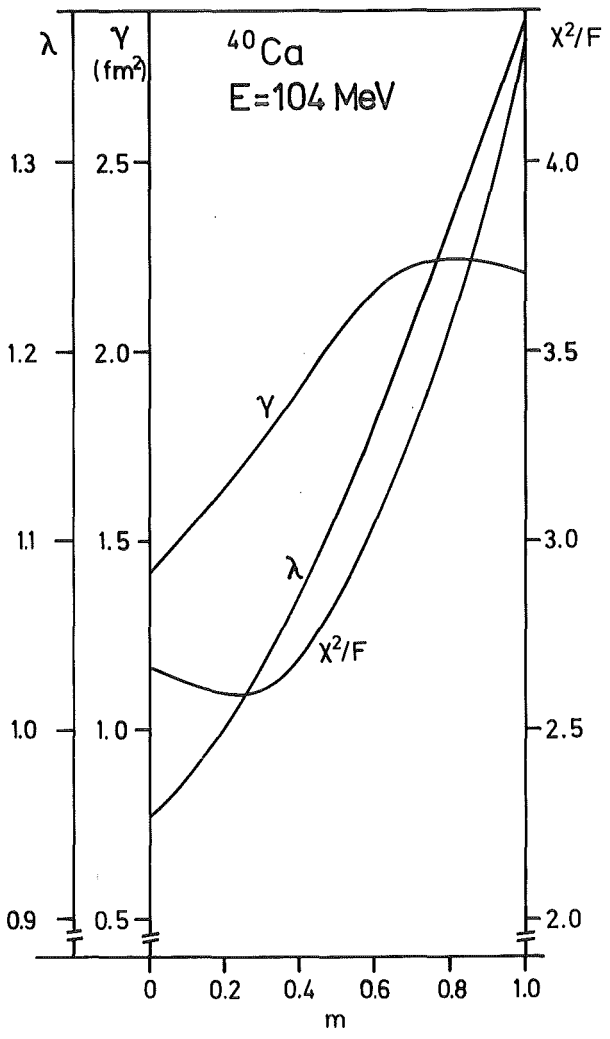

Fig. 3 Correlations between the parameters λ, γ, m of the density-dependent part of $V_{\alpha N}$ keeping the density-independent part fixed and corresponding values of χ^2/F.

^{42,44,48}Ca are presented in Table 2a. Only the imaginary part (WS-shape) of the optical potential was fitted to the data. For comparison also the integral quantities of the corresponding FB-potentials [12] are shown. In contrast to the ^{40}Ca case we observe a considerably worse reproduction of the experimental cross sections (characterized by the value of χ^2/F) and of the characteristic quantities of the optical potentials as obtained by the FB-method. The general trend of a decreasing value of χ^2/F when going from the LDA of form (5a) to (5c) or (6), respectively, is observed also for ^{42,44,48}Ca. The bad agreement of the folding model results with the phenomenological description may have different reasons originating either from the adopted nuclear matter densities [21] or from the effective interactions $V_{\alpha N}$ used. Out of the latter one reason may be concerned with the (widely used) assumption that the effective interaction should be constant at least for a limited range of nuclei. This must certainly be required for the density-independent part $f(|\vec{x}|)$ (eq.3). For the density-dependent part $v_{DD}(\rho_m)$, however, one can expect small changes between different nuclei due to the main origins of the density-dependence. These are Pauli-forbidden intermediate states in the Brueckner reaction matrix and knock-on exchange terms of the Fock type [17,18] which both are correlated to the nuclear structure and, therefore, may change. To account for such changes of the density-dependence in a phenomenological way followed here, the parameters γ and/or λ (eq. 4a) may be changed for different nuclei. Hence, γ was adjusted to the experimental cross sections in a best-fit procedure yielding the results compiled in Table 2b. The fit to the data and the reproduction of the "model-independent" FB-potentials is much better with this additional degree of freedom, as expected. The deviation of the optimized γ-values from the initial ones is larger than the errors of the parameters obtained from the fits which are of the order of 0.005. However, the γ-values are fairly inside the limits discussed above (c.f. Fig. 3). It should be noted that in all approaches γ increased for ^{42,44}Ca as compared to the values obtained from ^{40}Ca (c.f. Table 1) and decreased for ^{48}Ca. Increasing γ i.e. stronger density dependence was also found for other nuclei investigated (see Appendix A). Simply minded one can correlate these changes with the shell structure of the nucleus considering that ^{48}Ca is assumed to be a "better" closed shell nucleus than ^{40}Ca.

Table 2a Volume integrals J and rms-radii of the folded real optical potentials (v) and of WS imaginary potentials (w) using the effective interactions from Table 1 as compared to the phenomenological FB-potentials

Target	LDA eq.	χ^2/F	γ (fm^2)	$-J_v/4A$ (MeV fm^3)	$\langle r^2 \rangle_v^{1/2}$ (fm)	$-J_w/4A$ (MeV fm^3)	$\langle r^2 \rangle_w^{1/2}$ (fm)
^{42}Ca	(FB)	2.6	-	316 ± 3	4.37 ± 0.03	110.	4.93
	5a	10.5	2.136	317	4.39	105.	4.95
	5b	9.9	1.800	317	4.40	106.	4.93
	5c	9.0	1.382	320	4.39	108.	4.92
	6	8.6	1.645	320	4.39	108.	4.92
^{44}Ca	(FB)	2.7	-	314 ± 3	4.404 ± 0.03	112.	4.96
	5a	7.8	2.136	316.	4.43	108.	5.01
	5b	7.1	1.800	316.	4.43	110.	4.99
	5c	6.4	1.382	319.	4.43	112.	4.98
	6	6.1	1.645	318.	4.43	111.	4.98
^{48}Ca	(FB)	2.3	-	324 ± 5	4.51 ± 0.03	94.	5.11
	5a	8.5	2.136	306.	4.47	95.	5.11
	5b	7.6	1.800	310.	4.48	97.	5.10
	5c	5.6	1.382	315.	4.48	98.	5.06
	6	5.6	1.645	314.	4.48	98.	5.08

Table 2b: like Table 2a with the parameter γ optimized

Target	LDA eq.	χ^2/F	γ (fm^2)	$-J_V/4A$ (MeV fm^3)	$\langle r^2 \rangle_V^{1/2}$ (fm)	$-J_W/4A$ (MeV fm^3)	$\langle r^2 \rangle_W^{1/2}$ (fm)
^{42}Ca	5a	5.6	2.183	311	4.40	104.	4.98
	5b	5.0	1.852	312	4.41	106.	4.98
	5c	4.3	1.453	315	4.41	107.	4.96
	6	3.9	1.728	314	4.41	107.	4.96
^{44}Ca	5a	5.4	2.178	310	4.44	107.	5.03
	5b	5.0	1.844	312	4.45	110.	5.02
	5c	4.6	1.438	315	4.45	111.	5.01
	6	4.4	1.712	314	4.44	110.	5.01
^{48}Ca	5a	3.4	2.083	313	4.46	93.	5.09
	5b	3.4	1.750	315	4.46	96.	5.08
	5c	3.9	1.344	318	4.47	97.	5.07
	6	3.6	1.605	318	4.46	96.	5.07

Table 2 clearly supports also for nuclei other than the "calibration" nucleus ^{40}Ca that the different forms of the LDA (eqs. 5a-c, 6) are not equivalent and emphasizes the preference of the "mixed" LDA (eq. 6). A further confirmation of the latter form is found if flexible nuclear matter densities (FB-series) are introduced into the analyses which are fitted to the data keeping the effective interaction with the "mixed" LDA (m = 0.2) fixed. The results of such analyses taken from Ref. [12] are compiled in Table 3 demonstrating the full consistency of the folded optical potentials and the phenomenological FB-potentials (Tables 1,2). This result could not be reached with any of the other forms of the LDA for the various target nuclei analyzed as mentioned above.

Finally, we study the effect of the LDA for ^{40}Ca at another projectile energy (140 MeV) [14]. For this purpose the parameters of the density-independent part $f(|\vec{x}|)$ were taken from Table 1 as before and the parameters λ and γ have been varied in order to correct for the energy dependence of the effective interaction [17-20]. The results are compiled in Table 4 together with corresponding numbers of phenomenological analyses using the FB-potential [20]. Fully consistent with the results at E_α = 104 MeV we observe too a small volume integral for the real optical potential with LDA (5a) and (5b) which is partly compensated by the imaginary potential. The results for LDA (5c) and (6) are equivalent and approach the phenomenological FB-potentials closely confirming the findings for E_α = 104 MeV. The correlations between the parameters m, λ, γ as shown in fig. 4 for E_α = 140 MeV look very similar as for E_α = 104 MeV, (see fig. 3) in particular the nonlinear be haviour of γ for $m \gtrsim 0.4$ with a maximum of γ at m = 0.7 in reproduced.

The values of χ^2/F should also be compared with the value χ^2/F = 10.2 found in double-folding model analyses of the same data using the same nuclear density [10]. The corresponding integral moments of the double-folding real potentials and of the phenomenological imaginary potentials considerably deviate from the FB-potentials quoted in Table 4 [20] Values of $\chi^2/F \approx 1$ also quoted in Ref. [10] to be obtained by varying λ and introducing a squared WS-imaginary potential plus surface term seem dubious since the real potential deviated considerably from the

Table 3 Integral moments of folded optical potentials using the effective interaction from Table 1 (eq. 6) and "model-independent" FB-nuclear matter densities fitted to the data (Results taken from Ref. 12.)

Target	χ^2/F	$-J_v/4A$ (MeV fm^3)	$\langle r_v^2 \rangle^{1/2}$
^{40}Ca	2.1	320.5	4.350
^{42}Ca	2.8	316.7	4.397
^{44}Ca	2.8	312.0	4.416
^{48}Ca	2.3	319.6	4.485

Table 4 Results for ^{40}Ca(α,α) E_α = 140 MeV [14] taking parameters of $f(\vec{x})$ (eq. 3) from Table 1a

LDA eq.	χ^2F	λ	γ (fm^2)	$-J_v/4A$ (MeV fm^3)	$\langle r^2 \rangle_v^{1/2}$	$-J_w/4A$ (MeV fm^2)	$\langle r^2 \rangle_w^{1/2}$
(FB)	0.8	-	-	322 $\pm$ 3	4.41 $\pm$ 0.06	107.	4.88
5a	2.6	1.09	2.387	311	4.41	100.	4.92
5b	2.3	1.06	2.019	313	4.41	103.	4.90
5c	2.1	1.06	1.671	317	4.42	106.	4.87
6	2.1	1.07	1.980	317	4.42	106.	4.88

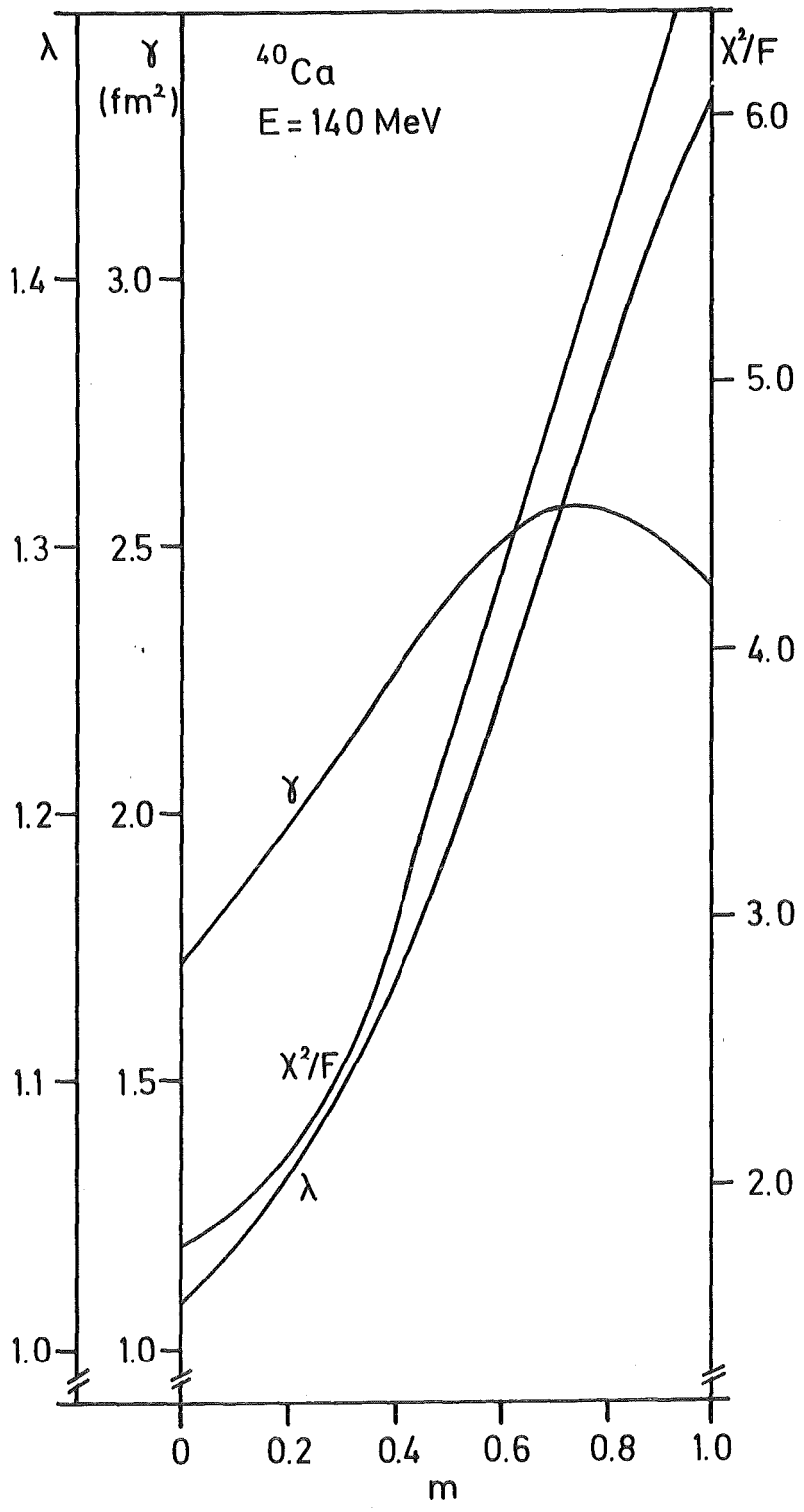

Fig. 4 Correlations between the parameters λ, γ, m for E_α = 140 MeV [14] .

"model-independent" FB-potential [20] in all cases. Introducing the revised imaginary potential forms in the present analyses (LDA: eq. 6) yielded only an improved value of $\chi^2/F = 2.0$ although here is much better agreement of the folded potential with the FB-potential than in Ref. [10].

5. Conclusion

The particular form of the LDA plays obviously an important role in single-folding model analyses of elastic α particle scattering in the region $E_\alpha = 100$ MeV and previously used assumptions about the equivalence of different forms should be revised. As demonstrated by the phenomenological potentials which are accurately determined by the experimental data also at small radii ($r \gtrsim 1.5$ fm) the α particles penetrate rather deep into the target nucleus during the scattering process. Consequently, it is most probable that the effective projectile-nucleon interaction depends not only on the density at the position of the interacting target nucleon but also on the density at the position of the α particle which may be different (at least at the nuclear surface) due to the rather long range of the effective αN-interaction. This is in agreement with double-folding model studies using different forms of the LDA [6]. The presented findings and suggestions - though being of semi-phenomenological character due to the choice of $f(|\vec{x}|)$ (eq. 3) - were shown to be relevant for different target nuclei and at different projectile energies. The full consistency in the values of χ^2/F and in size and shape of the potentials between the phenomenological and microscopic single-folding potentials using the suggested "mixed" LDA and the decoupling between the density-dependent and -independent parts of the effective interaction found for this form strongly confirm the validity of this approach for the determination of nuclear densities.

The author is grateful to Profs. E. Friedman and H. Rebel for valuable hints and claryfying discussions.

REFERENCES

[1] Jackson, D.F., Kembhavi, V.K.: Phys. Rev. 178, 1626 (1969)

[2] Bernstein, A.M.: Advances in Nucl. Phys. eds. M. Baranger and E. Vogt (Plenum Press, New York 1969)

[3] Rebel, H., Hauser, G., Schweimer, G.W., Nowicki, G., Wiesner, W., Hartmann, D.: Nucl. Phys. A218, 13 (1974)
Gils, H.J., Rebel, H., Buschmann, J., Klewe-Nebenius, H., Nowicki, G.P., Nowatzke, W.: Z. Phys. A - Atoms and Nuclei 279, 55 (1976)
Rebel, H.: Proc. EPS Conf. on Radial shape of nuclei (Cracow, Poland, 1976)

[4] Petrovich, F., Stanley, D., Bevelacqua, J.J.: Phys. Lett. 71B, 259 (1977)

[5] Majka, Z., Budzanowski, A., Grotowski, K., Strzalkowski, A.: Phys. Rev. C 18, 114 (1978)

[6] Majka, Z., Gils, H.J., Rebel, H.: Z. Phys. A - Atoms and Nuclei 288, 139 (1978)

[7] Satchler, G.R., Love, W.G.: Phys. Rep. 55, 183 (1979)

[8] Friedman, E., Gils, H.J., Rebel, H., Majka, Z.: Phys. Rev. Lett. 41, 1220 (1978)
Gils, H.J., Friedman, E., Majka, Z., Rebel, H.: Phys. Rev. C 21, 1245 (1980)

[9] Goldfarb, L.J.B., Nagel, P.: Nucl. Phys. A 341, 494 (1980)

[10] Kobos, A.M., Brown, B.A., Hodgson, P.E., Satchler, G.R., Budzanowski, A.: Nucl. Phys. A 384, 65 (1982)

[11] Gils, H.J., Friedman, E., Rebel, H., Buschmann, J., Zagromski, S., Klewe-Nebenius, H., Neumann, B., Pesl, R., Bechtold, G.: Phys. Rev. C21, 1239 (1980)
Pesl, R., Gils, H.J., Rebel, H., Friedman, E. Buschmann, J., Klewe-Nebenius, H., Zagromski, S.,Z.Phys. A- Atoms and Nuclei 313, 111 (1983)

[12] Gils, H.J., Rebel, H., Friedman, E.: Report KfK 3556 (1983) Kernforschungszentrum Karlsruhe (1983)

[13] Friedman, E., Batty, C.J.: Phys. Rev. C 17, 34 (1978)

[14] Goldberg, D.A., Smith, S.M., Burdzik, G.F.:
Phys. Rev. C 10, 1362 (1974)

[15] Friedman, E., Gils, H.J., Rebel, H.: Phys. Rev. C 24,
1551 (1982)

[16] Myers, W.D.: Nucl. Phys. A204, 465 (1973)

[17] Jeukenne, J.-P., Lejeune, A., Mahaux, C.:
Phys. Rev. C 16, 80 (1977)

[18] Jeukenne, J.-P., Mahaux, C.: Z. Phys. A - Atoms and Nuclei 302,
233 (1981)

[19] Srivastava, D.K., Ganguly, N.K., Basu, D.N.:
preprint (1983)

[20] Friedman, E., Gils, H.J., Rebel, H., Pesl, R.:
Nucl. Phys. A 363, 137 (1981)

[21] Brown, B.A., Massen, S.E., Hodgson, P.E.:
J. Phys. G 5, 1455 (1979)

[22] Gils, H.J.: Report KfK 3063, Kernforschungszentrum Karlsruhe
(1980)

[23] Majka, Z.: Phys. Lett. 76B, 161 (1978)

[24] Ray, L., Hoffmann, G.W., Barlett, M., McGill, J.,
Amann, J., Adams, G., Pauletta, G., Gazzaly, M.,
Blanpied, G.S.: Phys. Rev. C 23, 828 (1981)

Appendix

The influence of the LDA on Nuclear Matter Densities

In this Appendix the influence of the LDA on nuclear matter densities of different nuclei determined in the reversal use of the folding model is studied keeping the effective interaction fixed as obtained from ^{40}Ca. Since the studies are only for demonstration purposes the nuclear matter densities are parametrized by the Fermi-form

$$\rho_m(r) = \rho_o \cdot \left(1 + \exp \frac{r - c_m \cdot A^{1/3}}{a_m}\right)^{-1} \qquad (A - 1)$$

rather than by more advanced flexible forms like the FB-form [8, 11, 12]. The parameters of the effective interaction for the different forms of the LDA were taken from Table 1a without any change and the parameters c_m, α_m of the nuclear densities were varied in χ^2-fits together with the imaginary potential (WS-form). Results for the target nuclei $^{40,42,43,44,48}Ca$, ^{50}Ti, ^{52}V, ^{52}Cr are compiled in the following tables. For each form of the LDA the parameter γ was either adopted from Table 1a or optimized to fit the data. The parameter $\lambda = 1$ was not changed in any case. When comparing tables A1 to A4 it becomes obvious that the form of the LDA also influences the results nuclear matter densities considerably in this reversal use of the folding model. In same cases the changes are so large that one may doubt whether this method is at all capable to determine informations on size and shape of nuclei realiably. One should, however, note that by the present use of the folding model only *differences* between neighbouring nuclei can be determined due the "calibrated" effective interaction. These differences remain rather stable for any form of the LDA. In addition, there are the well-defined criteria provided by the FB-potential analyses to be used as measure for the relevance of the folding model approaches. Considering these criteria (in particular in connection with flexible FB-densities) the mixed LDA (eq. 6) is clearly favoured for all studied target nuclei [12] since only for this form full consistency is achieved between "model-independent" FB-potentials and single-folding semi-microscopic optical potentials (compare also Table 3).

Table A1 a:

Results of nuclear matter densities and optical potentials using LDA (N), Parameter γ fixed.

Target	χ^2/F	c_m (fm)	a_m (fm)	γ (fm^2)	$\langle r^2_v \rangle^{1/2}$ (fm)	$-J_v/4A$ (MeV·fm^3)	$\langle r^2_w \rangle^{1/2}$ (fm)	$-J_w/4A$ (MeV·fm^3)	$\langle r^2_m \rangle^{1/2}$ (fm)
^{40}Ca	3.34	1.066	0.496	2.136	4.346	317.1	4.942	99.0	3.372
^{42}Ca	7.69	1.029	0.532	2.136	4.408	312.2	4.988	102.5	3.405
^{43}Ca	2.60	1.061	0.500	2.136	4.402	312.9	4.995	102.9	3.427
^{44}Ca	6.00	1.032	0.518	2.136	4.419	306.2	5.002	105.1	3.417
^{48}Ca	3.15	1.133	0.436	2.136	4.477	317.6	5.118	95.2	3.578
^{50}Ti	2.24	1.081	0.466	2.136	4.487	303.7	5.053	91.3	3.538
^{51}V	4.61	1.080	0.499	2.136	4.561	311.5	5.122	89.7	3.614
^{52}Cr	2.13	1.091	0.436	2.136	4.484	298.0	5.091	96.3	3.547

Table A1 b:

As Table A1 a, parameter γ optimized

Target	χ^2/F	c_m (fm)	a_m (fm)	γ (fm^2)	$\langle r^2_v \rangle^{1/2}$ (fm)	$-J_v/4A$ (MeV·fm^3)	$\langle r^2_w \rangle^{1/2}$ (fm)	$-J_w/4A$ (MeV·fm^3)	$\langle r^2_m \rangle^{1/2}$ (fm)
^{40}Ca	3.34	1.066	0.496	2.136	4.346	317.1	4.942	99.0	3.372
^{42}Ca	4.16	1.165	0.410	2.274	4.394	310.9	4.963	106.7	3.487
^{43}Ca	2.52	1.078	0.486	2.151	4.401	313.2	4.996	103.5	3.438
^{44}Ca	3.39	1.178	0.385	2.276	4.414	307.9	4.975	110.4	3.526
^{48}Ca	2.73	1.065	0.504	2.076	4.485	317.6	5.115	94.4	3.534
^{50}Ti	1.75	1.147	0.403	2.199	4.493	305.6	5.053	93.5	3.601
^{51}V	2.16	1.200	0.372	2.233	4.557	314.1	5.111	93.1	3.714
^{52}Cr	1.71	1.057	0.467	2.101	4.481	297.0	5.091	95.0	3.514

Table A2 a:

Results as in Table A1 a using LDA (Nα/2), parameter γ fixed

Target	χ^2/F	c_m (fm)	a_m (fm)	γ (fm^2)	$\langle r^2_v \rangle^{1/2}$ (fm)	$-J_v/4A$ (MeV·fm^3)	$\langle r^2_w \rangle^{1/2}$ (fm)	$-J_w/4A$ (MeV·fm^3)	$\langle r^2_m \rangle^{1/2}$ (fm)
^{40}Ca	2.99	1.072	0.488	1.800	4.345	317.9	4.923	100.8	3.370
^{42}Ca	7.35	1.018	0.548	1.800	4.414	314.4	4.979	104.3	3.414
^{43}Ca	2.59	1.058	0.504	1.800	4.406	314.5	4.980	105.0	3.427
^{44}Ca	5.33	1.009	0.544	1.800	4.433	309.5	4.994	107.1	3.420
^{48}Ca	3.91	1.155	0.385	1.800	4.463	315.4	5.096	96.7	3.552
^{50}Ti	2.22	1.078	0.462	1.800	4.491	306.4	5.050	92.9	3.523
^{51}V	3.85	1.107	0.470	1.800	4.558	314.2	5.117	91.4	3.628
^{52}Cr	1.62	1.075	0.434	1.800	4.481	299.4	5.084	97.7	3.501

Table A2 b:

As Table A2 a, parameter γ optimized

Target	χ^2/F	c_m (fm)	a_m (fm)	γ (fm^2)	$\langle r^2_v \rangle^{1/2}$ (fm)	$-J_v/4A$ (MeV·fm^3)	$\langle r^2_w \rangle^{1/2}$ (fm)	$-J_w/4A$ (MeV·fm^3)	$\langle r^2_m \rangle^{1/2}$ (fm)
^{40}Ca	3.01	1.072	0.488	1.800	4.345	317.9	4.923	100.8	3.370
^{42}Ca	3.73	1.161	0.391	1.903	4.390	311.4	4.954	108.0	3.448
^{43}Ca	2.54	1.076	0.485	1.810	4.403	314.5	4.984	105.2	3.432
^{44}Ca	3.32	1.157	0.381	1.897	4.410	307.8	4.972	111.4	3.465
^{48}Ca	2.77	1.039	0.531	1.729	4.491	318.0	5.110	94.8	3.528
^{50}Ti	1.69	1.156	0.359	1.854	4.485	305.4	5.048	94.7	3.560
^{51}V	2.09	1.205	0.328	1.862	4.455	312.9	5.109	93.3	3.671
^{52}Cr	1.60	1.042	0.471	1.779	4.483	299.1	5.080	96.9	3.483

Table A3 a:

Results as in Table A1 a using LDA$^{\wedge}$(α), parameter γ fixed

Target	χ^2/F	c_m (fm)	a_m (fm)	γ (fm^2)	$\langle r^2_v \rangle^{1/2}$ (fm)	$-J_v/4A$ (MeV fm^3)	$\langle r^2_w \rangle^{1/2}$ (fm)	$-J_w/4A$ (MeV fm^3)	$\langle r^2_m \rangle^{1/2}$ (fm)
^{40}Ca	2.67	1.078	0.482	1.382	4.344	321.1	4.904	102.6	3.371
^{42}Ca	5.49	1.140	0.434	1.382	4.409	323.1	4.959	110.8	3.468
^{43}Ca	2.59	1.077	0.491	1.382	4.409	319.6	4.974	106.7	3.445
^{44}Ca	5.47	1.132	0.431	1.382	4.430	320.9	4.976	114.3	3.487
^{48}Ca	5.01	1.037	0.513	1.382	4.467	313.7	5.061	96.3	3.488
^{50}Ti	2.57	1.132	0.408	1.382	4.508	316.4	5.055	97.5	3.567
^{51}V	2.60	1.165	0.389	1.382	4.562	318.8	5.093	95.6	3.646
^{52}Cr	3.03	1.062	0.470	1.382	4.505	311.0	5.096	99.5	3.531

Table A3 b:

As Table A3 a, parameter γ optimized

Target	χ^2/F	c_m (fm)	a_m (fm)	γ (fm^2)	$\langle r^2_v \rangle^{1/2}$ (fm)	$-J_v/4A$ (MeV·fm^3)	$\langle r^2_w \rangle^{1/2}$ (fm)	$-J_w/4A$ (MeV·fm^3)	$\langle r^2_m \rangle^{1/2}$ (fm)
^{40}Ca	2.66	1.077	0.486	1.382	4.347	321.7	4.909	102.6	3.377
^{42}Ca	3.12	1.126	0.432	1.456	4.400	316.2	4.937	110.2	3.429
^{43}Ca	2.59	1.075	0.490	1.391	4.407	318.7	4.971	106.8	3.439
^{44}Ca	3.22	1.107	0.442	1.400	4.424	313.2	4.958	113.0	3.444
^{48}Ca	3.16	1.036	0.540	1.324	4.490	320.1	5.098	95.8	3.538
^{50}Ti	2.01	1.120	0.412	1.426	4.503	311.8	5.038	96.9	3.543
^{51}V	2.48	1.169	0.383	1.379	4.562	319.1	5.100	95.7	3.647
^{52}Cr	1.59	1.024	0.496	1.433	4.498	304.1	5.073	98.1	3.487

Table A4 a:

Results as in Table A1 a using LDA (M), parameter γ fixed, parameter m = 0.2

Target	χ^2/F	c_m (fm)	a_m (fm)	γ (fm^2)	$\langle r^2_v \rangle^{1/2}$ (fm)	$-J_v/4A$ (MeV fm^3)	$\langle r^2_w \rangle^{1/2}$ (fm)	$-J_w/4A$ (MeV fm^3)	$\langle r^2_m \rangle^{1/2}$ (fm)
^{40}Ca	2.80	1.071	0.490	1.645	4.344	320.1	4.901	102.6	3.371
^{42}Ca	5.59	1.140	0.435	1.645	4.406	322.7	4.958	110.4	3.470
^{43}Ca	2.57	1.067	0.500	1.645	4.407	318.4	4.973	106.4	3.440
^{44}Ca	5.36	1.126	0.439	1.645	4.426	319.9	4.971	113.8	3.484
^{48}Ca	5.84	1.072	0.471	1.645	4.457	313.0	5.062	97.4	3.490
^{50}Ti	2.33	1.123	0.418	1.645	4.502	314.5	5.051	96.7	3.563
^{51}V	2.40	1.171	0.381	1.645	4.557	318.0	5.096	95.4	3.649
^{52}Cr	2.32	1.051	0.478	1.645	4.498	308.1	5.087	98.8	3.519

Table A4 b:

As Table A4 a, parameter γ optimized

Target	χ^2/F	c_m (fm)	a_m (fm)	γ (fm^2)	$\langle r^2_v \rangle^{1/2}$ (fm)	$-J_v/4A$ (MeV fm^3)	$\langle r^2_w \rangle^{1/2}$ (fm)	$-J_w/4A$ (MeV fm^3)	$\langle r^2_m \rangle^{1/2}$ (fm)
^{40}Ca	2.80	1.071	0.490	1.645	4.344	320.1	4.901	102.6	3.371
^{42}Ca	3.15	1.133	0.426	1.721	4.398	315.8	4.938	109.9	3.438
^{43}Ca	2.57	1.075	0.490	1.653	4.405	317.9	4.405	106.7	3.439
^{44}Ca	3.19	1.115	0.436	1.726	4.420	312.4	4.420	112.6	3.451
^{48}Ca	3.26	1.054	0.519	1.568	4.484	320.6	5.104	96.2	3.537
^{50}Ti	1.92	1.106	0.431	1.680	4.498	310.6	5.043	96.1	3.541
^{51}V	2.75	1.646	0.399	1.646	4.556	317.4	5.090	95.6	3.642
^{52}Cr	1.66	1.022	0.497	1.683	4.491	302.8	5.075	97.8	3.486